Title	Analysis of Atmosphere Effect on Silicon Oxycarbide Synthesis with Controlled Chemical Compositions
Author(s)	Narisawa, Masaki; Funabiki, Fuji; Iwase, Akihiro; Wakai, Fumihiro; Hosono, Hideo
Editor(s)	
Citation	Journal of the American Ceramic Society. 2015, 98 (10), p.3373-3380
Issue Date	2015-10
URL	http://hdl.handle.net/10466/15579
Rights	This is the peer reviewed version of the following article: Narisawa M., Funabiki F., Iwase A., Wakai F., Hosono H. (2015), Effects of Atmospheric Composition on the Molecular Structure of Synthesized Silicon Oxycarbides, which has been published in final form at https://doi.org/10.1111/jace.13756. This article may be used for non-commercial purposes in accordance with Wiley Terms and Conditions for Self-Archiving.

Journal of the American Ceramic Society

Analysis of Atmosphere Effect on Silicon Oxycarbide Synthesis with Controlled Chemical Compositions

Journal:	*Journal of the American Ceramic Society*
Manuscript ID:	Draft
Manuscript Type:	Article
Date Submitted by the Author:	n/a
Complete List of Authors:	Narisawa, Masaki; Osaka Prefecture University, Graduate School of Engineering Funabiki, Fuji; Tokyo Institute of Technology, Materials & Structures Laboratory Iwase, Akihiro; Osaka Prefecture University, Graduate School of Engineering Wakai, Fumihiro; Tokyo Institute of Technology, Materials & Structures Laboratory Hosono, Hideo; Tokyo Institute of Technology, Materials & Structures Laboratory
Keywords:	silicon oxycarbide, thermodynamics, electron spin resonance, amorphous, pyrolysis

Analysis of Atmosphere Effect on Silicon Oxycarbide Synthesis with Controlled Chemical Compositions

Masaki Narisawa, Fuji Funabiki*, Akihiro Iwase, Fumihiro Wakai*, Hideo Hosono*

Graduate School of Engineering, Osaka Prefecture University, 1-1 Gakuen-Cho, Naka-Ku, Sakai, Osaka 599-8531, Japan

*Materials and Structures Laboratory, Tokyo Institute of Technology, 4259 Nagatsuta, Yokohama, 226-8503, Japan

Abstract

Densely cross-linked silicone resin particles with an averaged diameter of 2 μm were pyrolyzed in various atmospheres, such as hydrogen, argon and carbon dioxide in the temperature range of 700–1100 °C to obtain silicon oxycarbides. Residual masses of samples after pyrolysis were remained almost a constant at 700 °C notwithstanding that apparent colors were distinctly varied. The sample obtained in the H_2 atmosphere was white and that obtained in the CO_2 atmosphere was dark brown. Color of Ar sample at 700 °C was dark yellow. Beyond the pyrolysis temperature of 800 °C, Si–O–Si network evolution with free carbon segregation proceeded in the CO_2 atmosphere, whereas Si–C bond incorporation in main network was accelerated in the H_2 atmosphere. In the Ar atmosphere, both free carbon segregation and Si–C bond incorporation in the network occurred. In the samples obtained in the H_2 atmosphere, spin concentrations were in the range of 10^{16}–10^{17} g^{-1}, whereas those in the CO_2 and Ar were in the range of 10^{18}–10^{19} g^{-1}. Hydrogen capping of dangling bond formed during pyrolysis process was suggested.

I. Introduction

Silicon oxycarbides (Si–O–C) are amorphous materials in X-ray diffraction which are known to consist of SiO_xC_{4-x} (x=0–4) tetrahedral network usually including free carbon. For the synthesis, pyrolysis of polysiloxanes with suitable cross-linked structures is usually conducted.[1–4] Pyrolysis of condensates of Si alkoxide is also available, which is believed to be effective to control chemical compositions and nanostructures of the resulting materials.[5,6]

In classic works, main application of the silicon oxycarbides was components of ceramic base composites or binders of ceramics for high temperature uses.[7–9] In series of early works, porous Si–O–C ceramics with controlled foam morphology were successfully sythesized.[10,11]

On the other hand, various functional properties of Si–O–C ceramics begin to attract attentions in recent years. The polymer-derived Si–O–C anodes were found to offer a high reversible lithium storage capacity up to 920 mAh g^{-1}, whereas the theoretical capacity of conventional graphite anode is limited to 372 mAh g^{-1}.[12] Riedel et al. found piezoresistivity of hot pressed Si–O–C and proposed the application as pressure sensors available in severe environments.[13] Karakuscu et al. found that electric resistivity of porous Si–O–C were sensitively changed by partial pressures of gaseous species, such as NO_2, in environment.[14]

In addition, our group in Osaka Prefecture University succeeded in synthesis of Si–O–C(–H) ceramics with reduced carbon contents by using hydrogen for the pyrolysis process of silicone resin particles.[15] Transparent appearance of the obtained Si–O–C(–H) ceramics is highly attractive for optical uses, which could not be available in classic black Si–O–C ceramics. As expected from previous studies, these

Si–O–C(–H) ceramics exhibited even photoluminescence (PL) under excitation of UV light (350–370 nm).[16–20] The ceramics also possess unique oxidation resistance, which highly depends on the surface chemical nature.[21]

In the polymer precursor method for ceramic synthesis, control of starting molecular structures by organochemical technique has been a hot issue, and various polymers and resulting ceramic materials have been produced. They are now playing important roles in industry.[21–25] Effect of pyrolysis atmosphere on the resulting ceramic structures is, however, not clearly defined even at present. Using of hydrogen is known to diminish excess carbon in the resulting ceramics effectively.[15,26] Active filler method is known to be based on reaction of metal fillers with gaseous species in ambient atmosphere, and such reactions often yield dense ceramic composites with adopting suitable heat treatment conditions.[27] Changes in molecular structures and network evolution in the precursor during pyrolysis under influence of atmosphere, however, have not been sufficiently analyzed and discussed in previous studies. We selected commercialized silicon resin particles for the aimed study, although the molecular structure of the resin particles, mainly consisting of $(CH_3)SiO_3$ units, may be too simple as compared with most of the precursor polymers now developed and commercialized. Chemical composition, molecular structure, and particle size are, however, well controlled at the stage of the precursor synthesis. They can be regarded as standard for analyzing the atmosphere effect on resulting nature of the obtained Si–O–C or Si–O–C(–H) ceramics.

II. Experimental Procedure

The Si–O–C (or Si–O–C(–H)) ceramics for the study were synthesized from Tospearl 120 (Momentive Performance Materials Japan), which consisted of silicone

resin microspheres with an average diameter of 2 μm and with a chemical composition of $SiO_{1.66}C_{1.00}H_{3.36}$. Molecular structures and impurities in the precursor were analyzed in detail in previous studies.[15,20,21] 0.5–1.0 g of the precursor was placed on an alumina boat and heat-treated in an alumina tube at appointed temperatures of 700–1100 °C under a flow of hydrogen (H_2), argon (Ar) and carbon dioxide (CO_2). The heating rate up to the appointed temperatures was 200 °C/h and the holding time was 1h. Each gases were at an industrial grade (>99.9%). A H_2 flow rate was 1000 ml/min, whereas Ar and CO_2 gas flow rates were 300 ml/min. A 40 mm SSA alumina tube contained in a SiC heater furnace was used for pyrolysis, giving a flow rate of 800 and 240 mm/min, respectively.

FTIR spectra of pyrolysis products were obtained by Spectrum GX (PerkinElmer Japan Co., Ltd., Tokyo, Japan) with KBr pellet method. 32 scans were recorded for each sample and the background was subtracted. Residual spin concentrations in the pyrolyzed samples were estimated from signals obtained by EPR spectrometer of EMX8/2.7 (Bruker, Germany) using $CuSO_4$ $5H_2O$ as standard.

Elemental analysis were performed by ICP-AES analysis on Si by SPS 3529 UV (Hitachi High-Tech Science Corporation) and IR analysis on decomposition gas on C, O and H by TCH 600 and IR-412 (LECO corporation). Specific gravities of the pyrolyzed samples were measured by a glass picnometer (5 ml) using pure water as medium. Thermogravimetric – differential thermal analysis (TG-DTA) was performed on each samples (10-20 mg) in dry air flow up to 1400 °C with a heating rate of 10 °C/min by using TG-DTA 320 system (Seiko instruments Inc.). SEM images of the each pyrolysis products were obtained by S-4500 (Hitachi).

Thermodynamic calculation of Si–O–C–H system was carried out by using the

software package CaTCalc_ver 1A pro (Materials Design Technology Co. Ltd. Tokyo, Japan).

III. Results and Discussion

Figure 1 shows residual mass of the precursor after pyrolysis at each temperature in various atmospheres. There is no difference in residual masses at 700 °C, which is 94–95%. In the H_2 gas flow, residual mass decreases rapidly at 700–900 °C and keeps steady values of 78–79 % at 900–1100 °C. In the Ar gas flow, the residual mass decreases at the same temperature region, and keeps steady values of 85–86 % at 900–1100 °C. The absolute residual masses of the H_2 samples are apparently lower than those of the Ar samples. On the other hand, a residual mass of the CO_2 sample shows a small gain at 700–800 °C, and turns to decrease beyond 800 °C. This suggests moderate oxidation of the precursor in a CO_2 gas flow. At low temperature region, Si atoms in the polymer network selectively capture oxygen, whereas methyl groups are not completely decomposed to CO. At high temperature region, carbonaceous domains derived from methyl groups begin to be oxidized to form CO. A double circle in Fig. 1 indicates the sample which heat-treated at 800 °C in a CO_2 gas flow and secondly heat-treated at 1100 °C in an Ar gas flow. Since carbonaceous domains are maintained, the residual mass keeps a high value as compared with that merely heat-treated in a CO_2 gas flow up to 1100 °C.

Effect of atmosphere on ceramization process appears not only in mass loss behavior but also in obvious color of the pyrolyzed samples. Figure 2 (a) and (b) show photo images of the pyrolyzed samples under visible light and UV light. Color of the H_2 samples keeps white appearance, whereas colors of the Ar and CO_2 samples are

intrinsically black at 800 and 1100 °C. On the other hand, color of Ar 700 is dark yellow and that of the CO_2 700 is brown.

Under the UV light, H_2 800 and H_2 1100 exhibit strong PL, as described in previous studies.[15,20] On the other hand, the Ar and CO_2 samples exhibit no PL at 800 and 1100 °C. H_2 700 and Ar 700 seem to exhibit very weak PL. In previous studies, such weak PL observed at an early stage of ceramization was suggested to have relationship with oxygen vacancies and mixed bond structures on teterahedral Si atoms in Si–O–C network.[19,28–30] In CO_2 700, however, there is no indication of the PL possibly because of relatively high oxygen partial pressure of the CO_2 atmosphere.

FTIR spectra of the pyrolyzed samples were obtained, and peak positions of Si–O–Si (or Si–O–C) stretching vibration are plotted against pyrolysis temperatures (Figure 3).[31,32] As the pyrolysis temperature increases, the peak position shifts to larger wavenumbers. The peak positions of the CO_2 samples are always larger than those of the Ar and a H_2 gas flow at the same pyrolysis temperature. The peak wavenumbers of the H_2 samples are a little smaller than those of the Ar samples in a temperature range of 700–900 °C. At 1000 and 1100 °C, however, the peak wavenumber of the H_2 sample exceeds that of the Ar sample.

The results shown in Fig.2 and 3 suggest that the pyrolysis atmosphere has influenced on molecular structure of pyrolyzed samples even at an early stage of the ceramization, although there is no substantial difference in the residual mass. Figure 4 (a) and (b) show FTIR spectra of the samples obtained at 700 °C. As expected, each spectrum feature is apparently various. In the FTIR spectrum of the H_2 700, sharp peaks assigned to Si–CH_3 groups (1250 cm^{-1} and 780 cm^{-1}) appear. Formation of Si–CH_2–Si bridges is also suggested from existence of shoulder at 840 cm^{-1}, which overlaps on the band of

Si–O–Si bending vibration (800 cm^{-1}).[31] The main Si–O–Si (Si–O–C) stretching vibration band seem to have a peak at 1050 cm^{-1} and a shoulder at 1150 cm^{-1}. Perhaps, silesquioxane cage structure is maintained in the H_2 atmosphere.[33] The spectrum feature of the Ar and CO_2 samples are similar to that of amorphous silica besides a very small spike assigned to Si–CH_3 group (1250 cm^{-1}). In the Ar and CO_2 samples, cage structure seems to be deconstructed. Apparent peak width of the CO_2 700 is, however, sharp as compared with that of the Ar 700.

Figure 5 (a) and (b) shows FTIR spectra of the samples obtained at 800 °C. The peaks assigned to Si–CH_3 groups almost disappear. Main bands in the spectra are assigned to the Si–O–Si stretching vibration (peak:1100–1040 cm^{-1}), the Si–O–Si bending vibration (peak: 800 cm^{-1}) and the Si–O–Si rocking (peak: 450 cm^{-1}), which are generally observed in FTIR spectra of amorphous silica.[31] The peak width of the stretching vibration band is wide in H_2 800 and is narrow in CO_2 800. In Fig. 5 (b), the spectrum of H_2 800 exhibits an apparent shoulder at 880 cm^{-1}, which can be assigned to inorganic Si–C bonds incorporated in Si–O–C network.[34,35] This shoulder, however, does not appear in the spectra of Ar 800 and CO_2 800.

Table 1 shows elemental compositions and specific gravities of the Si–O–C(–H) ceramics after pyrolysis. Elemental compositions of the H_2 samples and the Ar samples were picked up from the data of our previous study, ref. 15. Therefore, hydrogen contents of H_2 1100 and Ar 1100 may be a little underestimated, because holding time of 3h was adopted in the previous study for the pyrolysis at 1100 °C. The Si, O and C molar ratios are, however, considered to be same.

At 800 °C, hydrogen contents of the samples are high, and the materials hold organic nature partly. At 1100 °C, hydrogen contents are reduced and dense ceramics are

obtained. H_2 1100 possesses near stoichiometric SiO_2–xSiC composition with no excess carbon or silicon. On the other hand, CO_2 1100 and CO_2 800–Ar 1100 possess near stoichiometric SiO_2–xC composition with no silicon carbide phase. Ar 1100 possesses phase combination of SiO_2–xSiC–yC. Specific gravity of H_2 1100 and Ar 1100 exceeds 2.2. Relatively high specific gravities of these materials probably correspond to Si–C bond incorporation in amorphous network. On the other hand, specific gravities of CO_2 1100 and CO_2 800–Ar 1100 are below 2.2. These measured values are acceptable because possible component phases in the samples are considered to be amorphous silica (specific gravity of 2.2) and carbon (specific gravity of 1.8–2.1).

Figure 6 (a) shows ESR signals of the H_2 1100 and CO_2 1100. The g-factor and linewidth of and ESR signal for H_2 1100 are estimated to be 2.0021 and 0.11 mT, whereas those of CO_2 1100 are 2.0024 and 0.35 mT. It is plausible that these spins exist on carbon atoms in the synthesized materials, because the estimated g-factors are consistent with those of the carbon dangling bonds in silicon carbides or carbonaceous materials.[36–39] The signal intensity and linewidth of the CO_2 1100 are far larger than those of H_2 1100. The large linewidth of the CO_2 1100 is probably controlled by spin-spin interaction in the system. On the other hand, Fig. 6 (b) shows spin concentrations of the samples pyrolyzed in H_2, Ar and CO_2. The spin concentrations of the H_2 samples are always 2–4 order magnitudes lower than those of the Ar or the CO_2 samples. The Ar samples and the CO_2 samples give an order of 10^{19} g^{-1} in a temperature range of 800–1100 °C. This spin concentration is almost the same as the values observed in previous studies of Si–C or Si–C–O samples derived from polycarbosilane in an Ar gas flow.[40,41] It means that the spin concentration mainly depends on the pyrolysis atmosphere, whereas the effect of structure and composition of precursor is

relatively minor. In the H_2 samples flow, spin concentration increase at 700–800 °C. Relatively high spin concentrations (10^{17} g^{-1}) are maintained at 800 and 900 °C. It, however, turns to decrease at 1000 °C.

Figures 7 (a)–(c) show SEM images of the pyrolysis products at 800 °C. Each particle holds independent shape and there is no apparent differences caused by pyrolysis atmosphere. The average diameters of the particles derived from the SEM images are 1.92±0.21 μm for H_2 800, 1.86±0.29 μm for Ar 800 and 2.06±0.25 μm for CO_2 800. Relatively large diameter of CO_2 may correspond to the highest residual mass after pyrolysis. The standard deviations of the analyzed values are large for further speculation.

Figure 8 (a) and (b) show results of TG-DTA analysis of the samples pyrolyzed at 1100 °C in various atmosphere. H_2 1100 exhibits mass gain under air flow beyond 800 °C, whereas CO_2 1100 exhibits mass loss beyond 1000 °C. CO_2 800–Ar 1100 also exhibits mass loss in an air flow. The starting point of the mass loss, however, shifts to lower temperature and absolute mass loss rate becomes large.

The observed mass gain of H_2 1100 can be assigned to oxidation of Si–C bonds, in which carbon exits as sp^3 carbon.[21] Although white Si–O–C(–H) is intrinsically amorphous, oxidation is defined in terms of the chemical reaction, $SiC + 2O_2 \rightarrow SiO_2 + CO_2$, in this case. From the chemical composition of H_2 1100 ($SiO_{1.54}C_{0.26}H_{0.12}$), we can expect a theoretical mass gain of 7.4% after the complete oxidation.

On the other hand, mass losses of CO_2 1100 and CO_2 800–Ar 1100 can be assigned to oxidation of sp^2 carbon domains trapped in amorphous silica. From chemical compositions of CO_2 1100 ($SiO_{2.02}C_{0.18}$) and CO_2 800-Ar1100 ($SiO_{1.97}C_{0.54}H_{0.07}$), we can expect mass losses of –4.0% for CO_2 1100 and –9.2% for CO_2 800–Ar 1100. These

expected values are well consistent with the observed TG curves. On the other hand, Ar 1100 does not show any mass change in appearance. It is, however, not probable that Ar 1100 has extremely high oxidation resistance. Perhaps, mass gain caused by sp^3 carbon oxidation is compensated by mass loss caused by sp^2 carbon oxidation.[6] In DTA curves (Fig. 8 (b)), all the samples exhibit exothermic reaction beyond 800 °C, reaction heat is largest in CO_2 800–Ar1100 and that is smallest in H_2 1100.

From the experimental results of FTIR spectra, elemental analysis and TG-DTA curves, it can be almost confirmed that hydrogen removes excess carbon effectively during pyrolysis whereas Si–C bond is incorporated in the formed network.

Figure 9 (a) and (b) show results of thermodynamic calculation of stable solid phases in precursor ($SiO_{1.66}C_{1.00}H_{3.36}$) – xH_2 combination systems under 1 bar pressure. If there is no additional hydrogen in the system (Fig. 9 (a)), stable phase combination is SiO_2–SiC–C in whole temperature range. The content of excess carbon depends on temperature that the system reaches equilibrium. At higher temperature, phase combination becomes to contain a larger amount of excess carbon. If $25H_2$ is introduced in the system (Fig. 9 (b)), SiO_2–SiC phase combination is stable up to 820 °C, whereas SiO_2–SiC–C combination becomes stable beyond 820 °C. It means that a large amount of hydrogen is necessary for decarbonization and decarbonization process must be finished at relatively low temperature.

Such thermodynamic calculations were, however, performed by assuming known stable crystalline phases in the Si, O and C systems. Nonetheless, Gibbs energy differences between condensed phases are generally small at the same elemental compositions, whereas gaseous phase gives large influence on Gibbs energy. In our consideration, it is appropriate to analyze the decarbonization process of the organic

Si–O–C–H system in terms of thermodynamic calculations by assuming well known crystalline phases as the starting components. Moreover, it is possible that amorphous Si–O–C–(H) ceramics is easily formed in given conditions as compared with mixture of the solid phases. Navrotsky et al. have estimated thermodynamic stabilities of white Si–O–C(-H) ceramics and found that the ceramics have negative enthalpies of formation compared to crystalline equivalents containing a mixture of phases, such as SiO_2 (cristobalite), SiC and C (graphite).[42,43]

On the other hand, Fig. 10 shows the case of 1 CO_2 introduction in the precursor. In this case, stable phase combination is SiO_2–C, and SiC phase does not exist in the calculated stable phases. As the temperature increases, the excess carbon content decreases. This means that a small amount of CO_2 introduction is suitable to achieve SiO_2–C composition. At high temperature, excess carbon phase, once formed, should be removed by oxidation in terms of the chemical reaction of $CO_2 + C \rightarrow 2CO$.

In addition, theses thermodynamic calculations do not cover information of elemental chemical reactions how organic silicone resin starts to react with H_2 or CO_2 during the ceramization. In a previous study of an early stage of decarbonization (750–850 °C) using H_2, we observed formation of many Si–CH_2–Si bridges and evidence of oxygen vacancies with neighborhood lone pair on Si atoms (ODC II).[30] Perhaps, such oxygen vacancies and the Si–CH_2–Si bridges accelerated Si–C bond incorporation process. On the other hand, spins in organic materials often play an important role in condensation reaction of organic species as cross-linker or polymerization initiator. Absence of the spins in the H_2 samples may contribute the rapid decarbonization process by inhibiting condensation reactions of organic species derived from methyl groups.

In the CO_2 samples, elemental chemical reaction is supposed to be CO_2 attack on organic polysiloxane network, which form rigid Si–O–Si bridges, whereas methyl groups are effectively converted to carbonaceous domains. A relatively high spin concentration in the CO_2 samples as well as the Ar samples may indicate role of spin in formation of carbonaceous domains composed of polycyclic aromatic hydrocarbons. This issue of elemental reaction between CO_2 and polysiloxane, however, needs further analysis at present.

In the Ar samples, formation of Si–CH_2–Si bridges is not apparent at 800 °C. High specific gravity of Ar 1100 and existence of SiC solid phase in the chemical composition analysis suggest that Si–C bonds are incorporated in formed network not only in the H_2 samples but also in the Ar samples. Perhaps, system under an Ar gas needs high temperature for Si–C bond incorporation. Since the spin concentration is high and hydrogen partial pressure is low, the excess carbon precipitation process is not inhibited in the Ar samples. The partial pressures of oxygen and hydrogen in the system are, however, almost randomly changed during the pyrolysis. The ceramization process of the precursor in an Ar gas flow contains complicated factors to be analyzed in spite of the simplicity at a glance.

VI. Conclusion

By using the same precursor, rather different amorphous ceramics can be synthesized by controlling partial pressure of hydrogen, oxygen or carbon in an ambient atmosphere during pyrolysis. Morphology of the obtained ceramics particles is almost the same, but the chemical composition is fairly different. In a H_2 atmosphere, excess carbon removal and inorganic Si–C bond incorporation are accelerated. These behaviors are well

consistent with phase equilibrium in a low temperature range thermodynamically calculated. On the other hand, close relationship with residual spins and excess carbon formation process is suggested. Low residual spin concentrations of the H_2 samples suggest that polymerization of organic species which would be converted to carbonaceous domains during pyrolysis is prevented in a hydrogen rich environment. In an Ar atmosphere, absence of sufficient hydrogen in the system yields excess carbon. Si–C bond incorporation in the main network is suggested to proceed at relatively high temperatures beyond 800 °C. Residual spin concentration is high which possibly has relationship with carbonaceous domain formation in the obtained ceramics. In a CO_2 atmosphere, Si atoms in the precursor are subjected to partial oxidation even at 700 °C. Since CO_2 700 exhibits dark color, even embryo of carbonaceous domains has already formed at 700 °C. Residual mass after pyrolysis is extremely high at 800 °C. The obtained ceramics beyond 800 °C, however, does not hold any Si–C bonds in the system.

Acknowledgements

We would like to thank Mr. Takafumi Tai for his effort in the laboratory of Graduate School of Engineering, Osaka Prefecture University. This work is partly supported by Collaborative Research Project of Materials and Structures Laboratory, Tokyo Institute of Technology.

References

[1]G. T. Burns, R. B. Taylor, Y. Xu, A. Zangvil, and G. A. Zank, "High-Temperature Chemistry of the Conversion of Siloxanes to Silicon Carbide," *Chem. Mater.*, **4**, 1313–23 (1992).

[2]F. I. Hurwitz, P. Heimann, S. C. Farmer, and D. M. Hembree Jr., "Characterization of the Pyrolytic Conversion of Polysilsesquioxanes to Silicon Oxycarbides," *J. Mater. Sci.*, **28**, 6622–30 (1993).

[3]G. M. Renlund, S. Prochazka, and R. H. Doremus, "Silicon Oxycarbide Glasses: Part I. Preparation and Chemistry," *J. Mater. Res.*, **6**, 2716–22 (1991).

[4]G. M. Renlund, S. Prochazka, and R. H. Doremus, "Silicon Oxycarbide Glasses .2. Structure and Properties," *J. Mater. Res.*, **6**, 2723–34 (1991).

[5]G. D. Soraru, G. D'Andrea, R. Campostrini, F. Babonneau, and G. Mariotto, "Structural Characterization and High-Temperature Behavior of Silicon Oxycarbide Glasses Prepared from Sol—Gel Precursors Containing Si H Bonds," *J. Am. Ceram. Soc.*, **78**, 379–87 (1995).

[6]C. M. Brewer, D. R. Bujalski, V. E. Parent, K. Su, and G. A. Zank, "Insights into the Oxidation Chemistry of SiOC Ceramics Derived from Silsesquioxanes. *J. Sol-Gel Sci. Technol.*, **14**, 49–68 (1999).

[7]F. I. Hurwitz, L. Hyatt, J. Gorecki, and L. D'Amore, "Silsesquioxanes as Precursors to Ceramic Composites," *Ceram. Eng. Sci. Proc.*, **8**, 732–43 (1987).

[8]F. I. Hurwitz, J. Z. Gyekenyesi, and P. J. Conroy, "Polymer-Derived Nicalon/Si-C-O Composites: Processing and Mechanical Behavior," *Ceram. Eng. Sci., Proc.*, **10**, 750–63 (1989).

[9]G. T. Burns, C. K. Saha, G. A. Zank, H. A. Freeman, "Polysilacyclobutasilazanes: Pre-ceramic Polymers for the Preparation of Sintered Silicon Carbide Monoliths," *J. Mater. Sci.*, **27**, 2131-40 (1992).

[10]P. Colombo and M. Modesti, "Silicon Oxycarbide Ceramic Foams from a Preceramic Polymer, *J. Am. Ceram. Soc.*, **82**, 573–78 (1999).

[11]Y.-W. Kim, S. H. Kim, C. Wang, and C. B. Park, "Fabrication of Microcellular Ceramics Using Gaseous Carbon Dioxide," *J. Am. Ceram. Soc.*, **86**, 2231–3 (2003).

[12]W. B. Xing, A. M. Wilson, K. Eguchi, G. Zank, and J. R. Dahn, "Pyrolyzed Polysiloxanes for Use as Anode Materials in Lithium-Ion Batteries," *J. Electrochem. Soc.*, **144**, 2410–6 (1997).

[13]R. Riedel, L. Toma, E. Janssen, J. Nuffer, T. Melz, and H. Hanselka, "Piezoresistive Effect in SiOC Ceramics for Integrated Pressure Sensors," *J. Am. Ceram. Soc.*, **93**, 920–4 (2010).

[14]A. Karakuscu, A. Ponzoni, P. R. Aravind, G. Sberveglieri, and G. D. Soraru, "Gas Sensing Behavior of Mesoporous SiOC Glasses," *J. Am. Ceram. Soc.*, **96**, 2366–9 (2013).

[15]M. Narisawa, S. Watase, K. Matsukawa, T. Dohmaru, and K. Okamura, "White Si–O–C(–H) Particles with Photoluminescence Synthesized by Decarbonization Reaction on Polymer Precursor in a Hydrogen Atmosphere," *Bull. Chem. Soc. Japan*, **85**, 724–726 (2012).

[16]I. Menapace, G. Mera, R. Riedel, E. Erdem, R.-A. Eichel, A. Pauletti, and G.A. Appleby, "Luminescence of Heat-treated Silicon-Based Polymers: Promising Materials for LED Applications," *J. Mater. Sci.*, **43**, 5790–6 (2008).

[17]Y. Ishikawa, A. V. Vasin, J. Salonen, S. Muto, V. S. Lysenko, A. N. Nazarov, N.

Shibata, and V.-P. Lehto, "Color Control of White Photoluminescence from Carbon-Incorporated Silicon Oxide," *J. Appl. Phys.*, **104**, 083522 (2008).

[18]A. Karakuscu, R. Guider, L. Pavesi, and G. D. Soraru, "White Luminescence from Sol–Gel-Derived SiOC Thin Films," *J. Am. Ceram. Soc.*, **92**, 2969-2974 (2009).

[19]S. Gallis, V. Nikas, H. Suhag, M. Huang, and A. E. Kaloyeros, "White Light Emission from Amorphous Silicon Oxycarbide(a-SiC_xO_y) Thin Films: Role of Composition and Postdeposition Annealing," *Appl. Phys. Lett.*, **97**, 081905 (2010).

[20]M. Narisawa,T. Kawai, S. Watase, K. Matsukawa, T. Dohmaru, K. Okamura, and A. Iwase, "Long-Lived Photoluminescence in Amorphous Si–O–C(–H) Ceramics Derived from Polysiloxanes," *J. Am. Ceram. Soc.,* **95**, 3935–3940 (2012).

[21]M. Narisawa, K. Terauds, R. Raj, Y. Kawamoto, T. Matsui, and A. Iwase, "Oxidation Process of White Si–O–C(–H) Ceramics with Various Hydrogen Contents," *Scripta Materialia*, **69**, 602-605 (2013).

[22]S. Yajima, J. Hayashi, and M. Imori, "Continuous Silicon Carbide Fiber of High Tensile Strength," *Chem. Lett.*, **4**, 931–4 (1975).

[23]R. Riedel, A. Kienzle, W. Dressler, L. Ruwisch, J. Bill, and F. Aldinger, "A Silicoboron Carbonitride Ceramic Stable to 2,000°C," *Nature*, **382**, 796–8 (1996).

[24]I. L. Rushkin, Q Shen, S. E. Lehman, and L. V. Interrante, "Modification of a Hyperbranched Hydridopolycarbosilane as a Route to New Polycarbosilanes," *Macromolecules*, **30**, 3141–46 (1997).

[25]P. Colombo, G. Mera, R. Riedel, and G. D. Soraru, "Polymer-Derived Ceramics: 40 Years of Research and Innovation in Advanced Ceramics," *J. Am. Ceram. Soc.*, **93,** 1805–37 (2010).

[26]M. Takeda, A. Saeki, J. Sakamoto, Y. Imai, and H. Ichikawa, "Effect of Hydrogen

Atmosphere on Pyrolysis of Cured Polycarbosilane Fibers," *J. Am. Ceram. Soc.*, **83**, 1063–9 (2000).

[27]P. Greil, "Active-Filler-Controlled Pyrolysis of Preceramic Polymers," *J. Am. Ceram. Soc.*, **78,** 835–48 (1995).

[28]L. Skuja, "Optically Active Oxygen-Deficiency-Relarted Centers in Amorphous Silicon Dioxide," *J. Non-Cryst. Solids.*, **239**, 16–48 (1998).

[29]L. Ferraioli, D. Ahn, A. Saha, L. Pavesi, and R. Raj, "Intensely Photoluminescent Pseudo-Amorphous SiliconOxyCarboNitride Polymer–Ceramic Hybrids," *J. Am. Ceram. Soc.*, **91**, 2422–4 (2008).

[30]M. Narisawa, T. Kawai, S. Watase, K. Matsukawa, and A. Iwase, "Investigation of Photoluminescence of Si−O−C(−H) Ceramics at an Early Stage of Decarbonization by using High Energy Excitation," *AIP Advances*, **4**, 017118 (2014).

[31]J. T. Fitch, G. Lucovsky, E. Kobeda, and E. A. Irene, "Effects of Thermal History on Stress‐Related Properties of Very Thin Films of Thermally Grown Silicon Dioxide," *J. Vac. Sci. Technol. B*, **7**, 153–162 (1989).

[32]A. Grill and D. A. Neumayer, "Structure of Low Dielectric Constant to Extreme Low Dielectric Constant SiCOH Films: Fourier Transform Infrared Spectroscopy Characterization," *J. Appl. Phys.*, **94**, 6697–6707 (2003).

[33]M. J. Loboda, C. M. Grove, and R. F. Schneider, "Properties of a-SiO_x:H Thin Films Deposited from Hydrogen Silsesquioxane Resins," *J. Electrochem. Soc.*, **145**, 2861–2866 (1998).

[34]G. Das, P. Bettotti, L. Ferraioli, R. Raj, G. Moriotto, L. Pavesi, and G.D. Soraru, "Study of the Pyrolysis Process of an Hybrid $CH_3SiO_{1.5}$ Gel into a SiCO Glass," *Vib. Spectrosc.*, **45**, 61–68 (2007).

[35]M. A. Mazo, A. Tamayo, F. Rubio, D. Soriano, and J. Rubio, "Effect of Processing on the Structural Characteristics of Sintered Silicon Oxycarbide Materials," *J. Non Cryst. Solids*, **391**, 23–31 (2014).

[36]B. L. V. Prasad, H. Sato, T. Enoki, Y. Hishiyama, Y. Kaburagi, A. M. Rao, P. C. Eklund, K. Oshida, and M. Endo, "Heat-treatment effect on the nanosized graphite π-electron system during diamond to graphite conversion," *Phys. Rev. B,* **62**, 11209–11218 (2000).

[37]J. L. Cantin, H. J. Von Bardeleben, Y. Shishkin, Y. Ke, R. P. Devaty, and W. J. Choyke, "Identification of the Carbon Dangling Bond Center at the 4H-SiC=SiO2 Interface by an EPR Study in Oxidized Porous SiC," *Phys. Rev. Lett.*, 92, 015502, 4pp (2004).

[38]C. Glover, M. E. Newton, P. M. Martineau, S. Quinn, and D. J. Twitchen, "Hydrogen Incorporation in Diamond: The Vacancy-Hydrogen Complex," *Phys. Rev. Lett.*, **92,** 135502, 4pp (2004).

[39] J. L. Cantin, H. J. von Bardeleben, Yue Ke, R. P. Devaty, and W. J. Choyke, "Hydrogen passivation of carbon Pb like centers at the 3C- and 4 H-SiC/SiO_2 interfaces in oxidized porous SiC," *Appl. Phys. Lett.*, **88**, 092108, 3pp (2006).

[40]M. Sugimoto, T. Shimoo, K. Okamura, and T. Seguchi, "Reaction Mechanism of Silicone Carbide Fiber Synthesis by Heat Treatment of Polycarbosilane Fibers Cured by Radiation: II, Free Radical Reaction," *J. Am. Ceram. Soc.*, **78,** 1849–52 (1995).

[41]M. Narisawa, M. Shimoda, K. Okamura, M. Sugimoto, and T. Seguchi, "Reaction Mechanism of the Pyrolysis of Polycarbosilane and Polycarbosilazane as Ceramic Precursor," *Bull. Chem. Soc. Japan*, **68**, 1098–1104 (1995).

[42]T. Varga, A. Navrotsky, J. L. Moats, R. M. Morcos, F. Poli, K. Muller, A. Sahay, and

R. Raj, "Thermodynamically Stable $Si_xO_yC_z$ Polymer-Like Amorphous Ceramics," *J. Am. Ceram. Soc.*, **90**, 3213–9 (2007).

[43]A. H. Tavakoli, M. M. Armentrout, M. Narisawa, S. Sen and A. Navrotsky, "White Si–O–C Ceramic: Structure and Thermodynamic Stability," *J. Am. Ceram. Soc.*, **98**, 242–246 (2015).

Figure Captions

Figure 1. Residual mass of the samples pyrolyzed in various atmospheres.

Figure 2. Photo images of the samples pyrolyzed in various atmospheres; (a) under visible light, (b) under UV light.

Figure 3. Peak positions of Si–O–Si stretching vibration in FTIR spectra.

Figure 4. FTIR spectra of the pyrolyzed samples; (a) H_2 700, Ar 700 and CO_2 700 (2500–450 cm^{-1}), (b) H_2 700, Ar 700 and CO_2 700 (expanded, 1000–600 cm^{-1}).

Figure 5. FTIR spectra of the pyrolyzed samples; (a) H_2 800, Ar 800 and CO_2 800 (2500–450 cm^{-1}), (b) H_2 800, Ar 800 and CO_2 800 (expanded, 1000–600 cm^{-1}).

Figure 6. (a) ESR signals of H2 1100 (×10) and CO_2 1100, (b) Estimated spin concentrations of the samples pyrolyzed in various atmospheres.

Figure 7. SEM images of pyrolyzed samples, (a) H_2 800, (b) Ar 800. (c) CO_2 800.

Figure 8. TG-DTA curves of the samples pyrolyzed in various atmospheres; (a) TG curves. (b) DTA curves.

Figure 9. Thermodynamic calculation on stable solid phases in a temperature range of

400–1000 °C at a total pressure of 1 bar; (a) $SiO_{1.66}C_{1.00}H_{3.36}$ system, (b) $SiO_{1.66}C_{1.00}H_{3.36}$ –25 H_2 system.

Figure 10. Thermodynamic calculation on stable solid phases in a temperature range of 400–1000 °C at a total pressure of 1 bar with $SiO_{1.66}C_{1.00}H_{3.36}$ –CO_2 system.

Table 1 Chemical compositions of samples pyrolyzed in various atmospheres (The compositions of H_2 800, 1100 and Ar 800, 1100 are picked up from ref. 15).

Sample	Elemental Composition	Stable Phase Composition	Specific gravity
H_2 800	$SiO_{1.68\pm0.02}C_{0.48\pm0.01}H_{1.66\pm0.03}$	$(SiO_2)-0.19(SiC)-0.38(C)-1.98(H)$	×
Ar 800	$SiO_{1.73\pm0.02}C_{0.65\pm0.01}H_{0.78\pm0.03}$	$(SiO_2)-0.16(SiC)-0.60(C)-0.90(H)$	2.02
CO_2 800	$SiO_{2.06\pm0.02}C_{0.63\pm0.01}H_{0.62\pm0.03}$	$(SiO_2)-0.63(C)-0.06(OH)-0.56(H)$	2.09
H_2 1100	$SiO_{1.54\pm0.02}C_{0.26\pm0.01}H_{0.12\pm0.03}$	$(SiO_2)-0.30(SiC)-0.04(C)-0.16(H)$	2.36
Ar 1100	$SiO_{1.87\pm0.02}C_{0.37\pm0.01}H_{0.03\pm0.03}$	$(SiO_2)-0.07(SiC)-0.33(C)-0.03(H)$	2.28
CO_2 1100	$SiO_{2.02\pm0.02}C_{0.18\pm0.01}H_{<0.03}$	$(SiO_2)-0.18(C)<0.02(OH)$	2.12
CO_2 800-Ar 1100	$SiO_{1.97\pm0.02}C_{0.54\pm0.01}H_{0.07\pm0.03}$	$(SiO_2)-0.02(SiC)-0.53(C)-0.07(H)$	2.10

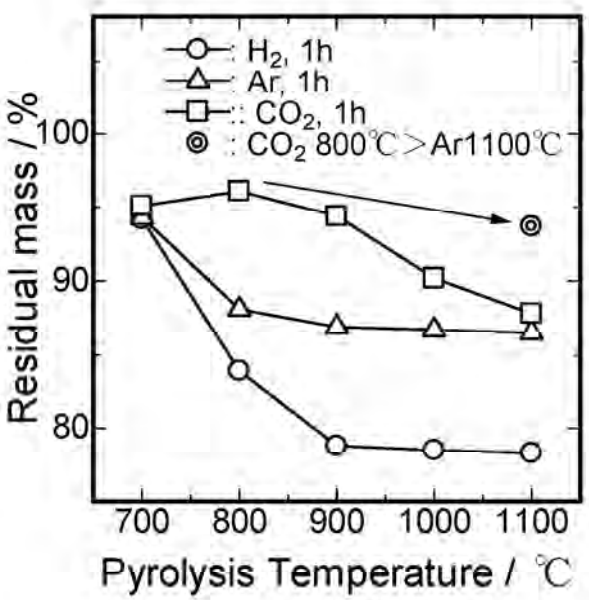

Figure 1. Residual mass of the samples pyrolyzed in various atmospheres.

210x297mm (300 x 300 DPI)

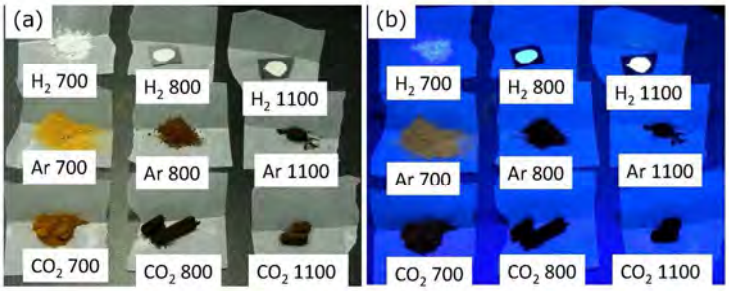

Figure 2. Photo images of the samples pyrolyzed in various atmospheres; (a) under visible light, (b) under UV light.

209x297mm (300 x 300 DPI)

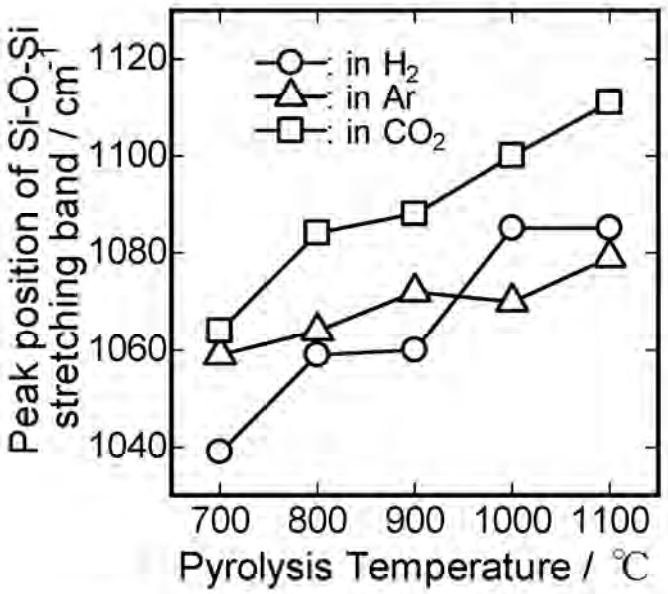

Figure 3. Peak positions of Si–O–Si stretching vibration in FTIR spectra.

210x297mm (300 x 300 DPI)

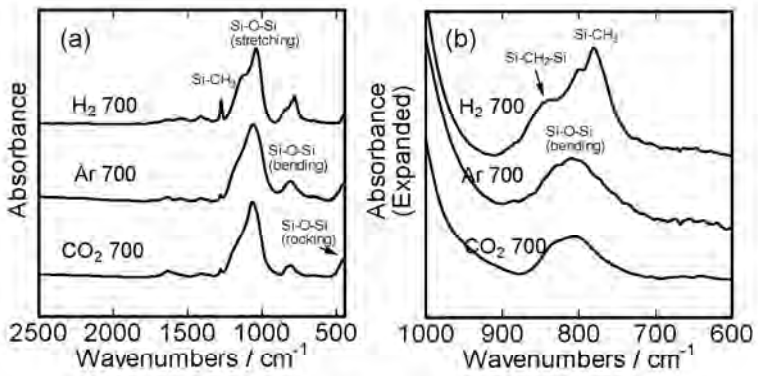

Figure 4. FTIR spectra of the pyrolyzed samples; (a) H_2 700, Ar 700 and CO_2 700 (2500–450 cm^{-1}), (b) H_2 700, Ar 700 and CO_2 700 (expanded, 1000–600 cm^{-1}).

210x297mm (300 x 300 DPI)

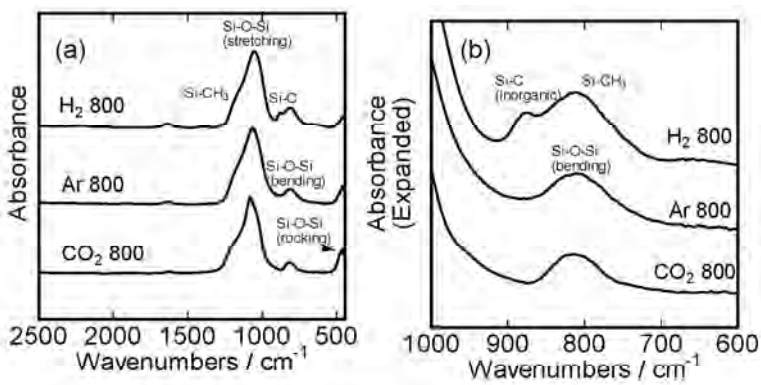

Figure 5. FTIR spectra of the pyrolyzed samples; (a) H_2 800, Ar 800 and CO_2 800 (2500–450 cm^{-1}), (b) H_2 800, Ar 800 and CO_2 800 (expanded, 1000–600 cm^{-1}).

210x297mm (300 x 300 DPI)

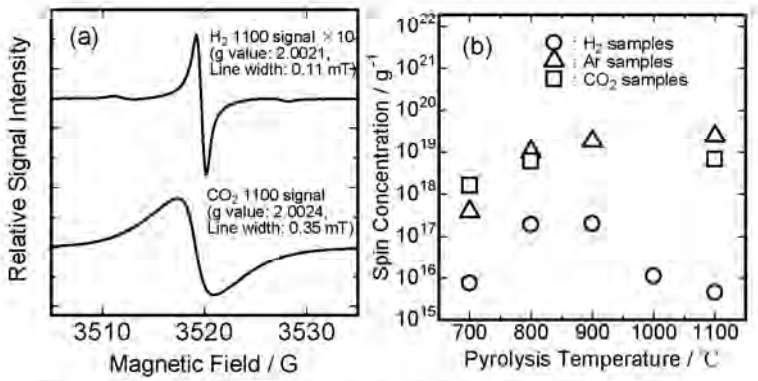

Figure 6. (a) ESR signals of H_2 1100 (×10) and CO_2 1100, (b) Estimated spin concentrations of the samples pyrolyzed in various atmospheres.

210x297mm (300 x 300 DPI)

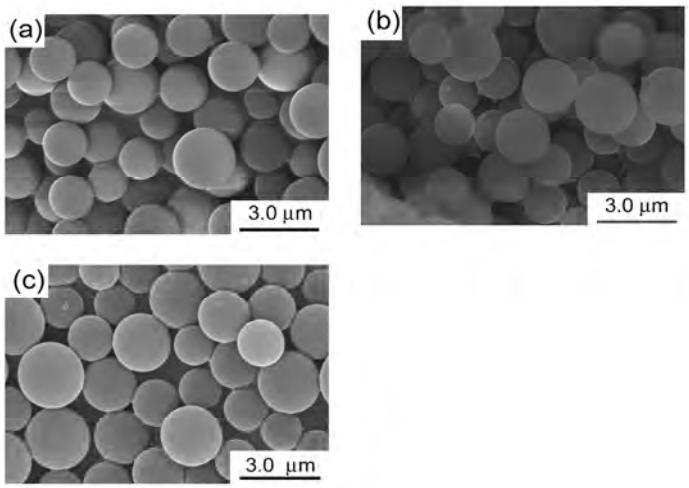

Figure 7. SEM images of pyrolyzed samples, (a) H_2 800, (b) Ar 800. (c) CO_2 800.

210x297mm (300 x 300 DPI)

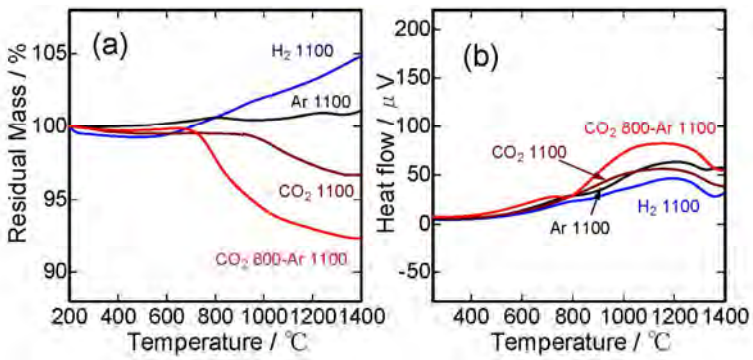

Figure 8. TG-DTA curves of the samples pyrolyzed in various atmospheres: (a) TG curves. (b) DTA curves.

210x297mm (300 x 300 DPI)

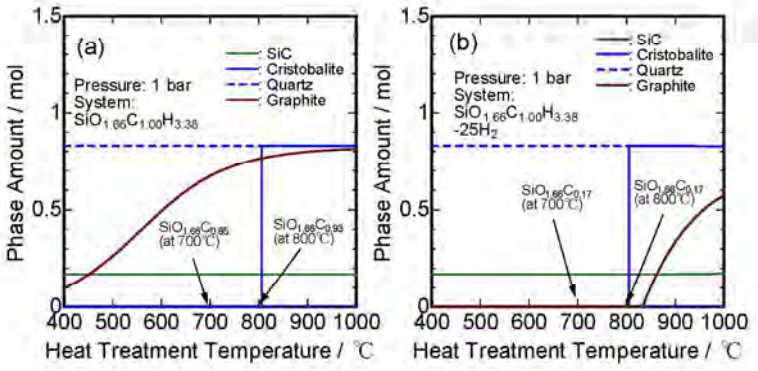

Figure 9. Thermodynamic calculation on stable solid phases in a temperature range of 400–1000 ° C, (a) $SiO_{1.66}C_{1.00}H_{3.36}$ system, (b) $SiO_{1.66}C_{1.00}H_{3.36}$ –25 H_2 system.

210x297mm (300 x 300 DPI)

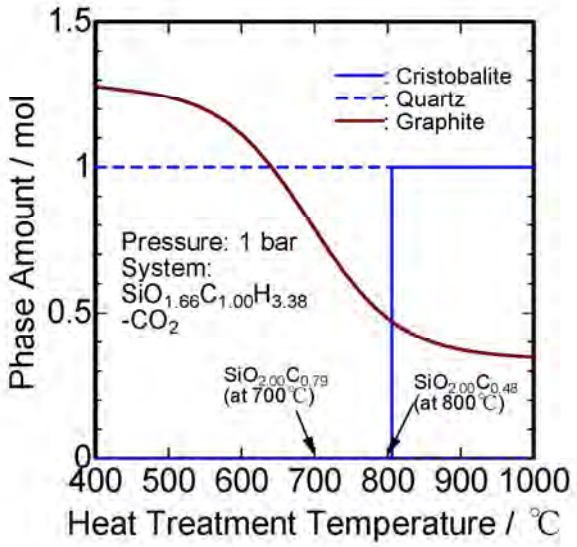

Figure 10. Thermodynamic calculation on stable solid phases in a temperature range of 400–1000 ° C in $SiO_{1.66}C_{1.00}H_{3.36}$ –CO_2 system.

210x297mm (300 x 300 DPI)

References

[1]G. T. Burns, R. B. Taylor, Y. Xu, A. Zangvil, and G. A. Zank, "High-Temperature Chemistry of the Conversion of Siloxanes to Silicon Carbide," *Chem. Mater.*, **4**, 1313–23 (1992).

[2]F. I. Hurwitz, P. Heimann, S. C. Farmer, and D. M. Hembree Jr., "Characterization of the Pyrolytic Conversion of Polysilsesquioxanes to Silicon Oxycarbides," *J. Mater. Sci.*, **28**, 6622–30 (1993).

[3]G. M. Renlund, S. Prochazka, and R. H. Doremus, "Silicon Oxycarbide Glasses: Part I. Preparation and Chemistry," *J. Mater. Res.*, **6**, 2716–22 (1991).

[4]G. M. Renlund, S. Prochazka, and R. H. Doremus, "Silicon Oxycarbide Glasses .2. Structure and Properties," *J. Mater. Res.*, **6**, 2723–34 (1991).

[5]G. D. Soraru, G. D'Andrea, R. Campostrini, F. Babonneau, and G. Mariotto, "Structural Characterization and High-Temperature Behavior of Silicon Oxycarbide Glasses Prepared from Sol—Gel Precursors Containing Si H Bonds," *J. Am. Ceram. Soc.*, **78**, 379–87 (1995).

[6]C. M. Brewer, D. R. Bujalski, V. E. Parent, K. Su, and G. A. Zank, "Insights into the Oxidation Chemistry of SiOC Ceramics Derived from Silsesquioxanes. *J. Sol-Gel Sci. Technol.*, **14**, 49–68 (1999).

[7]F. I. Hurwitz, L. Hyatt, J. Gorecki, and L. D'Amore, "Silsesquioxanes as Precursors to Ceramic Composites," *Ceram. Eng. Sci. Proc.*, **8**, 732–43 (1987).

[8]F. I. Hurwitz, J. Z. Gyekenyesi, and P. J. Conroy, "Polymer-Derived Nicalon/Si-C-O Composites: Processing and Mechanical Behavior," *Ceram. Eng. Sci., Proc.*, **10**, 750–63 (1989).

[9]G. T. Burns, C. K. Saha, G. A. Zank, H. A. Freeman, "Polysilacyclobutasilazanes: Pre-ceramic Polymers for the Preparation of Sintered Silicon Carbide Monoliths," *J. Mater. Sci.*, **27**, 2131-40 (1992).

[10]P. Colombo and M. Modesti, "Silicon Oxycarbide Ceramic Foams from a Preceramic Polymer, *J. Am. Ceram. Soc.*, **82**, 573–78 (1999).

[11]Y.-W. Kim, S. H. Kim, C. Wang, and C. B. Park, "Fabrication of Microcellular Ceramics Using Gaseous Carbon Dioxide," *J. Am. Ceram. Soc.*, **86**, 2231–3 (2003).

[12]W. B. Xing, A. M. Wilson, K. Eguchi, G. Zank, and J. R. Dahn, "Pyrolyzed Polysiloxanes for Use as Anode Materials in Lithium-Ion Batteries," *J. Electrochem. Soc.*, **144**, 2410–6 (1997).

[13]R. Riedel, L. Toma, E. Janssen, J. Nuffer, T. Melz, and H. Hanselka, "Piezoresistive Effect in SiOC Ceramics for Integrated Pressure Sensors," *J. Am. Ceram. Soc.*, **93**, 920–4 (2010).

[14]A. Karakuscu, A. Ponzoni, P. R. Aravind, G. Sberveglieri, and G. D. Soraru, "Gas Sensing Behavior of Mesoporous SiOC Glasses," *J. Am. Ceram. Soc.*, **96**, 2366–9 (2013).

[15]M. Narisawa, S. Watase, K. Matsukawa, T. Dohmaru, and K. Okamura, "White Si–O–C(–H) Particles with Photoluminescence Synthesized by Decarbonization Reaction on Polymer Precursor in a Hydrogen Atmosphere," *Bull. Chem. Soc. Japan*, **85**, 724–726 (2012).

[16]I. Menapace, G. Mera, R. Riedel, E. Erdem, R.-A. Eichel, A. Pauletti, and G.A. Appleby, "Luminescence of Heat-treated Silicon-Based Polymers: Promising Materials for LED Applications," *J. Mater. Sci.*, **43**, 5790–6 (2008).

[17]Y. Ishikawa, A. V. Vasin, J. Salonen, S. Muto, V. S. Lysenko, A. N. Nazarov, N.

Shibata, and V.-P. Lehto, "Color Control of White Photoluminescence from Carbon-Incorporated Silicon Oxide," *J. Appl. Phys.*, **104**, 083522 (2008).

[18]A. Karakuscu, R. Guider, L. Pavesi, and G. D. Soraru, "White Luminescence from Sol–Gel-Derived SiOC Thin Films," *J. Am. Ceram. Soc.*, **92**, 2969-2974 (2009).

[19]S. Gallis, V. Nikas, H. Suhag, M. Huang, and A. E. Kaloyeros, "White Light Emission from Amorphous Silicon Oxycarbide(a-SiC_xO_y) Thin Films: Role of Composition and Postdeposition Annealing," *Appl. Phys. Lett.*, **97**, 081905 (2010).

[20]M. Narisawa,T. Kawai, S. Watase, K. Matsukawa, T. Dohmaru, K. Okamura, and A. Iwase, "Long-Lived Photoluminescence in Amorphous Si–O–C(–H) Ceramics Derived from Polysiloxanes," *J. Am. Ceram. Soc.,* **95**, 3935–3940 (2012).

[21]M. Narisawa, K. Terauds, R. Raj, Y. Kawamoto, T. Matsui, and A. Iwase, "Oxidation Process of White Si–O–C(–H) Ceramics with Various Hydrogen Contents," *Scripta Materialia*, **69**, 602-605 (2013).

[22]S. Yajima, J. Hayashi, and M. Imori, "Continuous Silicon Carbide Fiber of High Tensile Strength," *Chem. Lett.*, **4**, 931–4 (1975).

[23]R. Riedel, A. Kienzle, W. Dressler, L. Ruwisch, J. Bill, and F. Aldinger, "A Silicoboron Carbonitride Ceramic Stable to 2,000°C," *Nature*, **382**, 796–8 (1996).

[24]I. L. Rushkin, Q Shen, S. E. Lehman, and L. V. Interrante, "Modification of a Hyperbranched Hydridopolycarbosilane as a Route to New Polycarbosilanes," *Macromolecules*, **30**, 3141–46 (1997).

[25]P. Colombo, G. Mera, R. Riedel, and G. D. Soraru, "Polymer-Derived Ceramics: 40 Years of Research and Innovation in Advanced Ceramics," *J. Am. Ceram. Soc.*, **93,** 1805–37 (2010).

[26]M. Takeda, A. Saeki, J. Sakamoto, Y. Imai, and H. Ichikawa, "Effect of Hydrogen

Atmosphere on Pyrolysis of Cured Polycarbosilane Fibers," *J. Am. Ceram. Soc.*, **83**, 1063–9 (2000).

[27]P. Greil, "Active-Filler-Controlled Pyrolysis of Preceramic Polymers," *J. Am. Ceram. Soc.*, **78,** 835–48 (1995).

[28]L. Skuja, "Optically Active Oxygen-Deficiency-Relarted Centers in Amorphous Silicon Dioxide," *J. Non-Cryst. Solids.*, **239**, 16–48 (1998).

[29]L. Ferraioli, D. Ahn, A. Saha, L. Pavesi, and R. Raj, "Intensely Photoluminescent Pseudo-Amorphous SiliconOxyCarboNitride Polymer–Ceramic Hybrids," *J. Am. Ceram. Soc.*, **91**, 2422–4 (2008).

[30]M. Narisawa, T. Kawai, S. Watase, K. Matsukawa, and A. Iwase, "Investigation of Photoluminescence of Si−O−C(−H) Ceramics at an Early Stage of Decarbonization by using High Energy Excitation," *AIP Advances*, **4**, 017118 (2014).

[31]J. T. Fitch, G. Lucovsky, E. Kobeda, and E. A. Irene, "Effects of Thermal History on Stress‐Related Properties of Very Thin Films of Thermally Grown Silicon Dioxide," *J. Vac. Sci. Technol. B*, **7**, 153–162 (1989).

[32]A. Grill and D. A. Neumayer, "Structure of Low Dielectric Constant to Extreme Low Dielectric Constant SiCOH Films: Fourier Transform Infrared Spectroscopy Characterization," *J. Appl. Phys.*, **94**, 6697–6707 (2003).

[33]M. J. Loboda, C. M. Grove, and R. F. Schneider, "Properties of a-SiO_x:H Thin Films Deposited from Hydrogen Silsesquioxane Resins," *J. Electrochem. Soc.*, **145**, 2861–2866 (1998).

[34]G. Das, P. Bettotti, L. Ferraioli, R. Raj, G. Moriotto, L. Pavesi, and G.D. Soraru, "Study of the Pyrolysis Process of an Hybrid $CH_3SiO_{1.5}$ Gel into a SiCO Glass," *Vib. Spectrosc.*, **45**, 61–68 (2007).

[35]M. A. Mazo, A. Tamayo, F. Rubio, D. Soriano, and J. Rubio, "Effect of Processing on the Structural Characteristics of Sintered Silicon Oxycarbide Materials," *J. Non Cryst. Solids*, **391**, 23–31 (2014).

[36]B. L. V. Prasad, H. Sato, T. Enoki, Y. Hishiyama, Y. Kaburagi, A. M. Rao, P. C. Eklund, K. Oshida, and M. Endo, "Heat-treatment effect on the nanosized graphite π-electron system during diamond to graphite conversion," *Phys. Rev. B,* **62**, 11209–11218 (2000).

[37]J. L. Cantin, H. J. Von Bardeleben, Y. Shishkin, Y. Ke, R. P. Devaty, and W. J. Choyke, "Identification of the Carbon Dangling Bond Center at the 4H-SiC=SiO2 Interface by an EPR Study in Oxidized Porous SiC," *Phys. Rev. Lett.*, 92, 015502, 4pp (2004).

[38]C. Glover, M. E. Newton, P. M. Martineau, S. Quinn, and D. J. Twitchen, "Hydrogen Incorporation in Diamond: The Vacancy-Hydrogen Complex," *Phys. Rev. Lett.*, **92,** 135502, 4pp (2004).

[39] J. L. Cantin, H. J. von Bardeleben, Yue Ke, R. P. Devaty, and W. J. Choyke, "Hydrogen passivation of carbon Pb like centers at the 3C- and 4 H-SiC/SiO_2 interfaces in oxidized porous SiC," *Appl. Phys. Lett.*, **88**, 092108, 3pp (2006).

[40]M. Sugimoto, T. Shimoo, K. Okamura, and T. Seguchi, "Reaction Mechanism of Silicone Carbide Fiber Synthesis by Heat Treatment of Polycarbosilane Fibers Cured by Radiation: II, Free Radical Reaction," *J. Am. Ceram. Soc.*, **78,** 1849–52 (1995).

[41]M. Narisawa, M. Shimoda, K. Okamura, M. Sugimoto, and T. Seguchi, "Reaction Mechanism of the Pyrolysis of Polycarbosilane and Polycarbosilazane as Ceramic Precursor," *Bull. Chem. Soc. Japan*, **68**, 1098–1104 (1995).

[42]T. Varga, A. Navrotsky, J. L. Moats, R. M. Morcos, F. Poli, K. Muller, A. Sahay, and

R. Raj, "Thermodynamically Stable $Si_xO_yC_z$ Polymer-Like Amorphous Ceramics," *J. Am. Ceram. Soc.*, **90**, 3213–9 (2007).

[43]A. H. Tavakoli, M. M. Armentrout, M. Narisawa, S. Sen and A. Navrotsky, "White Si–O–C Ceramic: Structure and Thermodynamic Stability," *J. Am. Ceram. Soc.*, **98**, 242–246 (2015).